Biochimica et Biophysica Acta, 985 (1989) 9–18
Elsevier

BBAMEM 74564

Electrical properties and molecular architecture of the channel formed by *Escherichia coli* hemolysin in planar lipid membranes

Monica Ropele and Gianfranco Menestrina

Dipartimento di Fisica, Università di Trento, I-38050 Povo, Trento (Italy)

(Received 29 March 1988)

Key words: Hemolysin; Ion channel; Single-channel current; Current-voltage characteristic; Phospholipid bilayer; Selectivity; pH dependence; (*E. coli*)

A 107 kDa hemolysin from *Escherichia coli* is able to open pores in lipid membranes. By studying its interaction with planar phospholipid bilayers we have derived some structural information on the organization of the pore. We measured the current-voltage characteristic and the ion selectivity of the channel both in neutral membranes, made of egg phosphatidylcholine (PC) and in negatively charged membranes, made of a 1:1 mixture of PC with phosphatidylserine (PS). Experiments were performed varying both the pH and the salt concentration of the bathing KCl solution. In neutral membranes the pore is ohmic and its conductance increases almost linearly with the salt concentration. The channel is cation-selective at high pH but nearly unselective at low pH. We interpret these results in terms of a minimal model based on classical electro-diffusional theories assuming that the pore is wide and bears a negative charge at its entrances. In membranes containing the acidic lipid the current-voltage curve is non-linear in such a way to suggest that the trans (but not the cis) entrance of the pore is affected by the surface potential of the membrane. Applying our model we find that the trans and cis entrances are located, respectively, about 0.5 nm and more than 5 nm apart from the plane of the membrane. We confirmed the asymmetric disposition of the channel by enzymatic digestion of preformed pores. This was effective only when the enzyme was applied on the cis side.

Introdcution

Escherichia coli is a frequent cause of such extraintestinal diseases in humans as infections of the urinary tract, pneumonia and meningitis, which may sometimes lead to severe forms of septicemia [1–3]. The immediate cause of these diseases is a protein toxin, 107 kDa in molecular weight, produced and secreted only by virulent strains of these bacteria [3–5]. This is commonly termed α-hemolysin or simply hemolysin.

E. coli hemolysin has been sequenced by genome decodification [6] and purified in large amounts from overproducing strains [4,7]. It causes hemolysis of red blood cells by a colloid osmotic shock due to the formation of hydrophilic pores in the cell membrane [8,9]. The properties of this ion-permeable channel can be conveniently studied in model systems such as planar phospholipid membranes [10,11], and small unilamellar vesicles [12].

The knowledge of the molecular mechanism controlling pore formation may help in designing effective strategies against the pathologies caused by this agent. Furthermore it is now becoming clear that several hemolysins produced by other Gram-negative bacteria (such as the *Proteus* family [13,14], *Morganella morganii* [13], *Bordetella pertussis* [15] and *Pasteurella haemolytica* [16]) are closely related to *E. coli* hemolysin. This protein may therefore be considered a prototype for a large group of bacterial toxins responsible for widespread diseases in humans and cattle.

In this paper we derive some structural information on the architecture of the pore formed by *E. coli* hemolysin by studying its electrical properties (such as selectivity and saturation) in planar lipid membranes.

Materials and Methods

Lyophilized *E. coli* hemolysin (donated by S. Bhakdi) was kept stored at −20°C and was stable for at least two months. After reconstitution in pure water its hemolytic activity was tested on rabbit erythrocytes as described in Ref. 8 and was usually 1000–2000 hemolytic units/ml (HU/ml). The molar concentration of the active toxin can be calculated from its hemolytic

Correspondence: G. Menestrina, Dipartimento di Fisica, Università di Trento, I-38050 Povo, Trento, Italy.

activity using the relation 1 HU/ml = 10^{-10} M determined by an ELISA assay (Bhakdi, S., personal communication).

Planar lipid bilayers were prepared by apposing two monolayers on a hole (0.2 mm in diameter) punched in a 12 μm thick Teflon septum which separates two buffered salt solutions [17]. The hole was pretreated with *n*-hexadecane and the monolayers were spread from a 10 mg/ml lipid solution in *n*-hexane as described [10,18]. Lipids used were saturated egg phosphatidylcholine (PC, by P.L.Biochemicals) either alone or in a 1 : 1 mixture with brain phosphatidylserine (PS, by Calbiochem). Both lipids were more than 99% pure.

E. coli hemolysin was added to only one of the solutions bathing a preformed stable bilayer (called the cis compartment). The current flowing through the membrane, under voltage clamp conditions, was sent to an *I–V* converter built around a virtual grounded operational amplifier (Burr Brown OPA 104C). The cis compartment was connected to the virtual ground and voltage signs referred to it. Current is defined as positive when cations flow into this compartment. The baseline conductance of the membranes did not exceed 50 pS. Ag|AgCl electrodes were used either directly immersed into the electrolyte solution, or (for the selectivity experiments) via agarose bridges.

The bathing solutions (4 ml on each side) contained appropriate concentrations of KCl (100 mM if not otherwise specified) and 5 mM of one of the following buffers: CAPS, Tris, Hepes, Mes or acetic acid, used in this order for pH values ranging from 11 to 4, and finally adjusted by suitable amounts of HCl or KOH. The pH was checked at the beginning and at the end of the experiment and in most cases did not change by more than 0.1 unit. Experiments were performed at room temperature.

Results

Single-channel properties in neutral membranes

Addition of small amounts of *E. coli* hemolysin (2 to 10 HU/ml) to the cis chamber of a voltage-clamped planar phospholipid membrane produces a current increase in uniform steps (Fig. 1A) which indicates the formation of ionic channels in the bilayer [10,18]. Pores which open at negative voltages (appearing as discrete downward deflections in the first part of the current trace) become closed again when positive voltages are applied (stepwards decreases of the current at +20 mV in the same trace).

Even at a negative voltage of −20 mV a single-channel transiently opens and closes (Fig. 1B); the time spent in the open state becomes longer the more negative the applied potential. A complete study of this voltage-dependent opening and closing behaviour, called

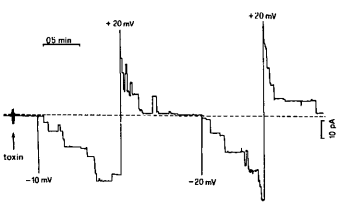

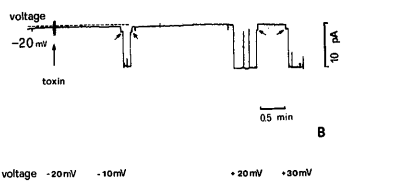

Fig. 1. Effects of *E. coli* hemolysin on the conductance of planar lipid bilayers. (A) Ionic current induced by *E. coli* hemolysin in a PC/PS bilayer formed in 50 mM KCl, 5 mM Hepes, pH 7.0. 3 HU/ml of hemolysin were introduced into the cis compartment where indicated. Downward deflections of the current trace, in steps of uniform size, appear approx. 20 seconds after the addition of the toxin. These steps are typically due to the opening of ionic channels into the membrane. A dashed line indicates zero of current. Changing the potential to +20 mV immediately closes all the channels. Pores open again at −20 mV and close at +20 mV. (B) Similar conditions as above but only 1 HU/ml of toxin was used and one single channel was seen for some time opening and closing. In between the closed and the open state (indicated by letters c and o, respectively) there is a substate of very small conductance and very short lifetime (indicated by arrows). Apparently, the pore always opens and closes via this substate. (C) Histograms representing the number of events with a given current amplitude observed in current traces like that in part A for different applied voltages. Mean current values can be obtained in this way which are then used to produce single-channel current-voltage curves.

'gating' of the channel, will be presented in a separate paper [19].

A closer inspection of single-channel recordings reveals the existance of an extra state in addition to the open and the closed one, indicated by arrows in the trace of Fig. 1B. However, the conductance of this state is so small (less than 10% of the open state conductance) and its lifetime so short that we have not considered it further.

From the discrete steps in current traces like that of Fig. 1A it is possible to derive the current flowing through the channel in the open state at any applied voltage and to build up histograms such as that in Fig. 1C.

The average current-voltage ($I-V$) curve of the single pore can be calculated from these histograms, Fig. 2A. In a neutral membrane the current-voltage characteristic is virtually ohmic (Fig. 2A) at any salt concentration. The conductance (slope of the $I-V$ curve) is roughly proportional to the ionic concentration of the KCl solution (Fig. 2B) with only a slight tendency to increase sublinearly (saturation).

As in the case of other channels [20–22] such nonlinearity suggests the presence of a fixed charge at the entrance of the pore, modulating the local ion concentrations. The strong cation selectivity of the channel at pH 7.0 (see Fig. 4) implicates that this charge is negative so that it locally accumulates cations and repels anions.

If this hypothesis is correct we expect that changing the pH of the solution will modify the charge at the pore entrance, and hence the conductance of the pore. This is indeed the case as shown in Fig. 3.

Effects of pH on the conductance and selectivity of the pore

Single channel current-voltage curves in a neutral membrane are shown in Fig. 3A, for different values of pH in a 0.1 M KCl solution. Increasing the pH increases the slope of the $I-V$ curve which otherwise remains linear. The calculated conductance is reported in Fig. 3B in a titration curve. The nearly linear increase of the conductance within the pH range 4.5 to 10.5 suggests that chemical groups of widely different nature contribute to building up the fixed charge of the pore. pH values outside this interval were not investigated because *E. coli* hemolysin failed to form channels into the membrane.

Another prediction of the fixed-charge hypothesis is that the cation selectivity of the pore is modulated by the pH of the solution, because it is due to counterion condensation on the negative charge. We verified that this is correct too.

The ion selectivity of the channel was determined in a 10-fold KCl gradient either by measuring the intersection of the single-channel $I-V$ curve with the voltage

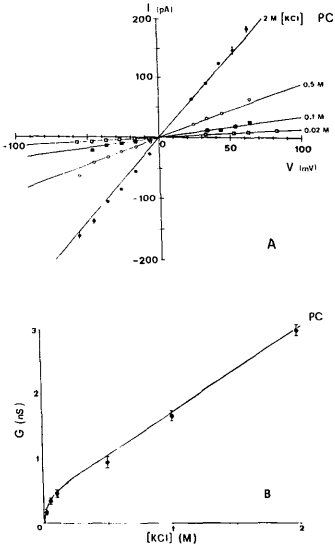

Fig. 2. Current-voltage characteristic of the *E. coli* hemolysin pore in neutral membranes. (A) Single-channel current, I, as a function of the applied voltage, V, in PC membranes separating symmetrical KCl solutions. Solutions contained the specified amount of KCl, 1 mM EDTA and 5 mM Hepes, pH 7.0. Each point is the average ± S.D. of at least 20 values obtained as in Fig. 1A during one experiment. Solid lines are the predictions of the electrostatic model described in the text with the parameters listed in Table II. (B) Single-channel conductance, G, vs. the concentration of the KCl solutions. G was determined as the slope of a current-voltage curve as in part A. All points are means ± S.D. of at least three independent determinations on different membranes. Solid line is the prediction of the model with the parameters in Table II.

axis (Fig. 4) or by finding the potential at which no current flows in membranes containing many channels [10,23]. Reversal voltages (V_{rev}) obtained by the two methods always agreed to within a few mV and were strongly dependent on the pH (Fig. 4B).

At high pH the channel was highly cation selective (indicated by a large positive value of V_{rev} close to that expected for ideal cation selectivity) but at pH 4.5 it became rather unselective (indicated by a V_{rev} proximal to zero). This is clear from the calculation of the relative permeability of K^+ with respect to Cl^- using to the

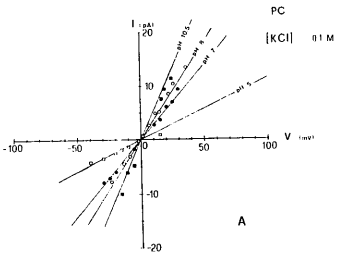

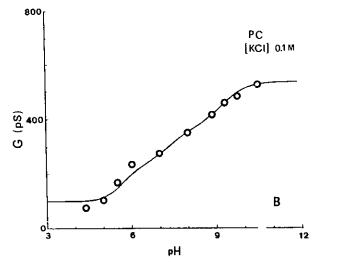

Fig. 3. Electrical properties of the *E. coli* hemolysin pore at different pH values. (A) Single-channel current-voltage characteristics as a function of the pH. PC membranes separated two symmetrical 100 mM KCl solutions buffered at different pH values as specified. The current-voltage curve is ohmic also in this case. Solid lines are the predictions of the model presented in the text with the parameters listed in Table II. (B) Single-channel conductance, G, vs. the pH of the KCl solution. G was determined as the slope of an $I-V$ curve as in part A. Solid line is the prediction of the model using the parameters in Table II. Other conditions as in Fig. 2.

Nernst equation [24] as reported in Table I. Within the pH interval under consideration this ratio changes from about one at pH 4.6 to about 24 at pH 8.7.

Effect of membrane surface potential on the $I-V$ curve of the pore

Interestingly we found that when the pores are inserted into a negatively charged bilayer (containing 50% of the acidic lipid PS) the current-voltage characteristic becomes non-linear (Fig. 5A). A change in the $I-V$ curve was not unexpected because the membrane surface potential is known to affect the current flowing through a pore if its entrance is located in close proximity of the plane of the membrane [25–27].

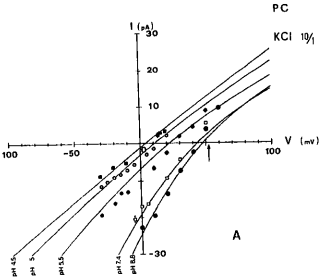

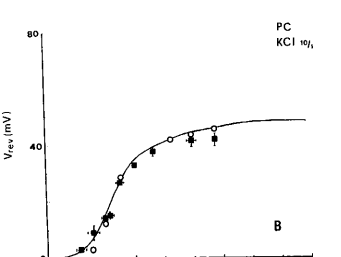

Fig. 4. Selectivity of the *E. coli* hemolysin pore in neutral membranes. (A) Single-channel current-voltage curves obtained in a PC membrane separating two asymmetrical solutions containing either 500 mM (cis side) or 50 mM (trans side) KCl, buffered as in Fig. 3. $I-V$ curves extrapolate at a positive voltage (V_{rev}) indicating a pH-dependent cation selectivity of the pore. Ideal cation selectivity under these conditions is indicated by an arrow. Solid lines are the predictions of the model with the parameters in Table II. (B) pH dependence of V_{rev} obtained as in part A (open symbols) or by the method of tail currents (closed symbols). Solid line is the prediction of the model using the parameters listed in Table II. Other conditions as in Fig. 2.

TABLE I

Effects of pH on the ion selectivity of the E. coli hemolysin pore

The ratio of the potassium permeability, $P(K^+)$, over the chloride permeability, $P(Cl^-)$, has been calculated from the reversal voltage (see Fig. 4) according to the Nernst equation [24].

pH	$P(K^+)/P(Cl^-)$
4.6±0.2	1.1±0.1
5.0±0.1	2.1±0.2
5.5±0.1	4.7±0.5
7.4±0.1	14.6±1.9
8.7±0.2	24.3±4.2

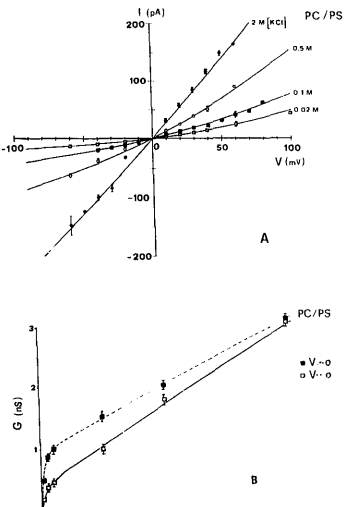

Fig. 5. Current-voltage characteristic of the *E. coli* hemolysin pore in negatively charged membranes. (A) $I-V$ characteristics in PC/PS membranes separating two symmetrical solutions containing the specified amount of KCl, 1 mM EDTA and 5 mM Hepes, pH 7.0. The current-voltage curve is nonlinear in this case. Solid lines are the predictions of the model with the parameters in Table II. (B) Single-channel conductance, G, vs. the concentration of the KCl solutions. G was determined as the slope of a current-voltage curve, as in part A, at either large positive (full symbols) or large negative (open symbols) applied potentials. Solid line is the same as in Fig. 2B, dashed line was drawn by eye. Other conditions as in Fig. 2.

Two values of the conductance can be derived in this case which correspond to the asymptotic slopes of the $I-V$ curve for large positive and large negative voltages, respectively (Fig. 5B). We found that the conductance at negative voltages is virtually the same as in neutral membranes whereas that at positive voltages is always larger. The difference becomes smaller as the ionic strength is increased.

Since the pore is substantially cation selective at neutral pH (see Table I), the larger current observed at positive potentials (when cations flow from the trans to the cis compartment) indicates that the trans entrance is located near the surface of the membrane. Here it experiences an increased concentration of cations due to the attractive surface potential of the bilayer. This effect is expected to decline at high ionic strength (as observed), because of the screening of the surface potential by counterions.

Also the fact that the current at large negative voltages (when cations flow from the cis to the trans compartment) is virtually the same in membranes with widely different surface potentials, indicates that the cis entrance of the pore is located sufficiently far from the plane of the membrane not to be influenced by its surface potential.

These two findings indicate a rather asymmetric disposition of the channel into the membrane suggesting that it protrudes on the cis side (from which the toxin has inserted into the bilayer) but not on the trans side.

To investigate this particular aspect further, we studied the effect of a proteolytic enzyme on membranes treated with the hemolysin. We found that trypsin is able to inactivate the channels when added to the cis compartment, while it is totally ineffective when added to the opposite side (Fig. 6).

This confirms that a large part of the toxin remains exposed on the membrane at the cis side, while no enzyme-sensitive group (essential for channel activity) protrudes on the opposite side.

Discussion

We now present a model based on well established electrochemical theories which can account for the electrical properties of the pore formed by *E. coli* hemolysin. The model assumes that all the channels are equal and independent and that each one is a hollow cylinder filled with water, with inner radius r and length l. Furthermore the pore has fixed charges at its entrances and is asymmetrically inserted into the bilayer so that it protrudes differently on the two sides of the membrane.

Effects of fixed charges at the pore entrances

The measurable quantity in our experiments is the current, I, flowing through the channel under different conditions (Fig. 1). The most general expression for this current is given by the Goldman-Hodgkin-Huxley (GHK) equation [24,28,29]:

$$I = \sum_i I_i \tag{1}$$

$$I_i = \frac{\pi r^2}{l} u_i \epsilon_0 z_i (V + \psi_T - \psi_C) \frac{\left[C_T^i e^{\frac{-z_i e_0}{kT}\psi_T} - C_C^i e^{\frac{-z_i e_0}{kT}(V+\psi_T)} \right]}{\left[1 - e^{\frac{-z_i e_0}{kT}(V+\psi_T-\psi_C)} \right]} \tag{2}$$

where i indicates the contribution of the ionic species

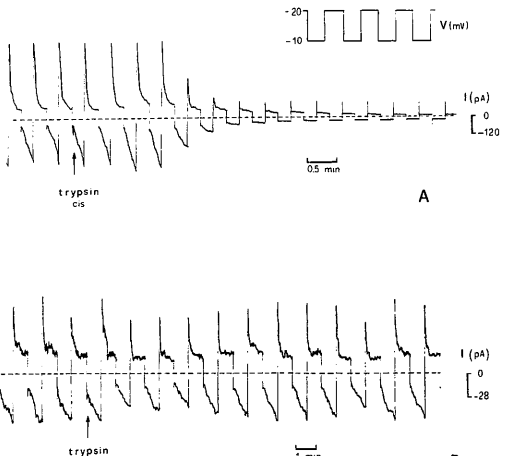

Fig. 6. Effects of tryptic digestion on the conductance induced by *E. coli* hemolysin. (A) *E. coli* hemolysin, 5 HU/ml, was added to a PC membrane and a continuous square wave was applied (the voltage jumped between −10 mV and +20 mV as indicated in the upper trace). After some time a dynamic equilibrium was reached, i.e., channel turned on at the negative voltage with a constant rate and turned off at the positive voltage with a defined time constant. Addition of trypsin, 9 U/ml, on the cis side, indicated by an arrow, produced the total disappearing of the hemolysin-induced conductance within 3 min. (B) In a similar experiment the conductance induced by 5 HU/ml of *E. coli* hemolysin was instead completely unaffected (for more than 30 min) by the addition of 13 U/ml of trypsin on the trans side.

present, i.e. K^+ and Cl^-, r and l the radius and length of the pore, u_i and z_i the mobility and valence of the ion i, C_C^i and C_T^i the bulk concentration of the ion i at the cis and trans sides, respectively, V the applied voltage, ψ_T and ψ_C the local potential at the trans and cis entrances, k Boltzmann constant, T abolute temperture and e_0 electronic charge.

For symmetric salt solutions

$$C_T^i = C_C^i = C^i \tag{3}$$

and introducing a constant:

$$A = \frac{\pi r^2 u_i e_0 z_i}{l} \tag{4}$$

Eqn. 2 reduces to:

$$I_i = A(V + \psi_T - \psi_C)C^i \frac{e^{\frac{-z_i e_0}{kT}\psi_T}\left(1 - e^{\frac{-z_i e_0}{kT}V}\right)}{\left(1 - e^{\frac{-z_i e_0}{kT}(V - \psi_T - \psi_C)}\right)} \tag{5}$$

which in general gives a non-linear dependence of the current I upon the voltage V.

The linearity of the current-voltage curve in neutral membranes (Fig. 2A and Fig. 3A) implies that the potentials at the two entrances of the pore are the same (within experimental resolution), that is:

$$\psi_T = \psi_C = \psi \tag{6}$$

Accordingly we obtain:

$$I_i = A \cdot C^i \cdot V \cdot e^{\frac{-z_i e_0}{kT}\psi} \tag{7}$$

If ψ were zero the conductance of the pore ($G = I/V$) whould increase linearly with the concentration of the salt, but we have observed that this is not the case (Fig. 2B). Furthermore since the pore is cation selective $I(K^+) > I(Cl^-)$ and we have to assume that ψ is negative from Eqn. 7.

A least-squares fitting of Eqn. 7 to the experimental curves of Fig. 2A allows us to estimate ψ as a function

of the salt concentration as reported in Fig. 7A. ψ is large at low ionic strength but decreases at high concentrations. This is what one should expect because the potential generated by fixed charges is screened by the counterions at high ionic strength.

A theoretical expression for ψ may be derived as described by Nelson and McQuarrie [30]. For a symmetric distribution of point charges (total charge being Q) located around the entrance of a pore of radius r the result is simply:

$$\psi_0 = \frac{2Q}{4\pi\varepsilon_r\varepsilon_0} \frac{e^{-\chi r}}{r} \tag{8}$$

with:

$$\chi^2 = \frac{N_0 e_0^2}{\varepsilon_r \varepsilon_0 kT} \sum_i C_i z_i^2 \tag{9}$$

where $\varepsilon_r\varepsilon_0$ is the dielectric constant of water and N_0 is Avogadro's number.

This expression is similar to the Debye-Hückel potential (in fact χ is the Debye-Hückel coefficient) generated by a single point charge in an electrolyte solution [31,32], except for a factor of two multiplying the charge. This is due to the fact that in our case the fixed charges are located at the boundary between a medium of low dielectric constant (the protein in the membrane) and one of high dielectric constant (the water solution) instead of being immersed in the latter.

It is advisable to introduce the usual correction into Eqn. 8 to take into account the finite dimensions of the counterions:

$$\psi = \psi_0 \frac{e^{\chi\delta}}{1+\chi\delta} \tag{10}$$

where δ is a typical length which for a KCl solution may be assumed to be 0.36 nm [31,32].

A least-squares fitting of Eqn. 10 to the experimental points of Fig. 7A allows us to calculate the total fixed charge on the entrance of the pore at pH 7.0 as -1.15 e_0. The estimated cross sectional area of the pore is about 10-times that of a gramicidin channel and 4-times that of the acetylcholine-receptor channel [33]. This prevents the flowing ions from interacting strongly with the walls of the pore and thus justifies the use of a simple diffusional model in our case.

Fixed charges on proteins are due to the presence of acidic and basic side chains on their amino acid residues. As such the total charge depends on the pH of the solution and in particular it is expected to become more negative at high pH and less negative at low pH. According to our model a larger value of the negative charge implies a larger entrance potential (Eqns. 8–10) and hence a larger current through the pore (Eqn. 7).

This is exactly what we have observed, Fig. 3. In general we may assume that the fixed charge depends on the pH of the solution according to:

$$Q = \sum_j \frac{Q_j}{1 + \frac{[H]}{K_j}} \tag{11}$$

where [H] is the concentration of protons and Q_j is the amount of fixed charge for which protons have a dissociation constant K_j.

Using Eqns. 7–11 it is possible to predict the dependence of the single-channel conductance on the pH of the solution, Fig. 3. A reasonable fit requires the use of three chemically different charges with distinct pK values, as reported in Table II.

Despite the fact that the effective pK of charged side chains on amino acid residues belonging to long polypeptide chains may be shifted more than one unit up or down compared to that of the pure amino acid in solution (because of the local environment, [34,35]), it is tempting to speculate that Q_1 is due to carboxyl groups on acidic residues (aspartate or glutamate), Q_2 is due to a histidine and Q_3 to a lysine.

It is evident from inspection of Eqns. 7–10 that in the present model the cation selectivity of the channel is a direct consequence of the fact that the fixed charge is negative, which makes $I(K^+)$ large and $I(Cl^-)$ small. Thus we expect that changing the fixed charge (e.g. by varying the pH) would also change the selectivity of the pore.

This is precisely what we have found in experiments in which a 10-fold KCl gradient was established across

TABLE II

Geometrical and chemical parameters defining the E. coli hemolysin pore

List of the best fit parameters used in the electrostatic model to describe the experiments in Figs. 2–5 and Fig. 7.

Definition	Symbol	Value	Units
Geometrical dimensions of the pore			
inner radius	r	0.6 ±0.1	nm
outer radius [a]	R	3.5 ±0.2	nm
length	l	12 ±1	nm
distance trans entrance	x_T	0.5 ±0.1	nm
distance cis entrance	x_C	≥ 5	nm
Chemical groups on the pore mouths			
Charge	Q_1	0.85±0.10	e.u. [b]
	Q_2	0.25±0.05	e.u.
	Q_3	0.20±0.05	e.u.
Cologarithm of dissociation constant	pK_1	5.3 ±0.1	
	pK_2	7.3 ±0.1	
	pK_3	9.2 ±0.1	

[a] Determined from the molecular weight of the toxin assuming a relative density of 0.8 for a protein.

[b] e.u., electronic units.

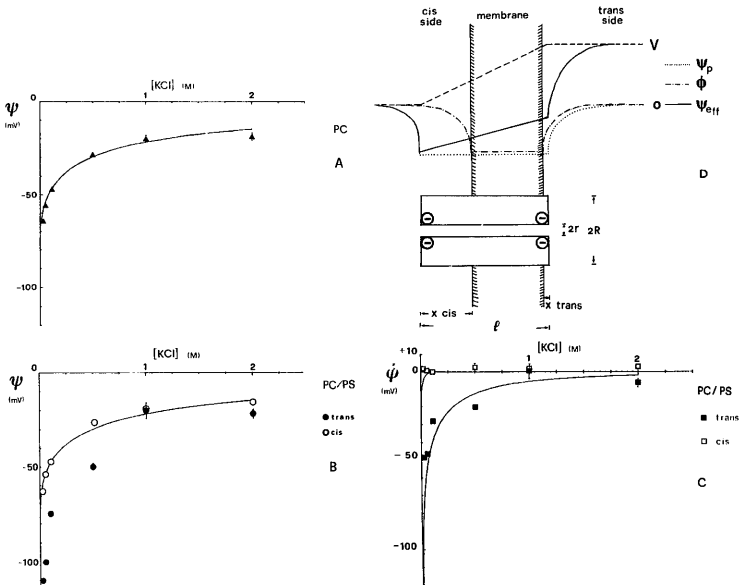

Fig. 7. Entrance potentials at the pore mouths. (A) Entrance potential at either of the two pore mouths was obtained by a least-squares adaptation of Eqn. 7 to the experimental points of Fig. 2, assuming for l a value ranging from 12 to 13 nm, which apply to the thickness of a lipid bilayer plus the distances of the two entraces of the pore from the plane of the membrane. Solid line is the prediction of Eqn. 10 of the model using the parameters listed in Table II. A pore diameter of 1.1–1.3 nm can be evaluated, which is not far from the evaluation of 2–3 nm derived from the study of the release of markers from erythrocytes [8]. (B) Entrance potentials at each of the two mouths of the pore when this is inserted into a negatively charged (PC/PS) membrane. ψ_T (full points) and ψ_C (open points) were obtained by a least squares fitting of Eqn. 5 (with the same fixed parameters as in part A) to the experiments of Fig. 5. Solid line is the same as in part A, i.e., ψ obtained in neutral membranes. (C) Contribution of the membrane surface potential ϕ to the entrance potential at the trans mouth (full symbols) or at the cis mouth (open symbols). ϕ was calculated subtracting ψ, as determined in part A, from ψ_T and ψ_C determined in part B. Solid lines are the predictions of the GCS equation [26,36] using the pertinent values for the surface charge of the PC/PS membrane [26,36,37] and the two mouth distances given in Table II. (D) Sketch of the pore with the definition of the geometrical parameters whose best fit values are given in Table II. The thick solid line is the effective potential profile, ψ_{eff}, seen by the ions moving through the pore resulting from the sum of three components: the applied potential, V (dashed line), the membrane potential ϕ (dashed-dotted line) and the pore potential ψ due to the fixed charges (dotted line).

the channel. Current-voltage curves in such asymmetrical conditions can be calculated, according to our model, by means of the more general Eqn. 2 with the condition 6 and the parameters already determined from experiments in the symmetric salt solutions (Figs. 2 and 3) which are reported in Table II. These predictions are shown in Fig. 4A as solid lines for different values of the pH. We feel that the fit between experimental points and theoretical expectations is quite good especially since there is no adjustable parameter in this plot.

The following expression for V_{rev} may be derived from Eqn. 2 setting $I = 0$:

$$V_{rev} = \frac{kT}{e_0} \ln \left(\frac{C_C^i + C_T^i \, e^{\frac{2e_0\psi_T}{kT}}}{C_T^i + C_C^i \, e^{\frac{2e_0\psi_T}{kT}}} \right) \qquad (12)$$

The prediction of Eqn. 12, using the parameters listed in Table II, is shown in Fig. 4B and compared with the experimental values determined either as in Fig. 4A (from single-channel experiments) or by the method of Ref. 23 (from many-channel experiments). The agreement is rather good and again we wish to emphasise that no adjustable parameter was present in this plot.

These findings demonstrate that our model can predict the results of experiments completely different from those used to derive it.

Effects of membrane surface potential

When *E. coli* hemolysin pores are inserted into a negatively charged membrane their current-voltage characteristic becomes asymmetrical, Fig. 5. This indicates that ψ_T and ψ_C are different in this case and hence that Eqn. 5 should be used to calculate the current flowing through the channel.

A least-squares fitting of Eqn. 5 to the experimental points of Fig. 5A allows us to derive the values of ψ_T and ψ_C for a negatively charged membrane as a function of the salt concentration. The results are shown in Fig. 7B; ψ_C virtually coincides with ψ as determined in neutral membranes, whereas ψ_T is considerably larger.

The simplest interpretation of these findings [25–27] is that the surface potential of the membrane does add, at the two entrances of the pore, to the potential generated by the pore itself.

We will call $\phi(x)$ the surface potential, with x indicating the distance from the plane of the membrane at which it is measured. The contribution of $\phi(x)$ to the entrance potential at the two pore mouths may be calculated by subtracting ψ (as it was measured in neutral membranes) from ψ_T and ψ_C.

These data are presented in Fig. 7C for different KCl concentrations. They indicate that $\phi(x)$ at the trans entrance declines when the ionic strength increases, whereas at the cis entrance it is always virtually zero.

A theoretical expression of $\phi(x)$ is given by the Gouy-Chapman-Stern (GCS) equation, as described for example in Refs. 26 and 36. Fitting of the GCS potential to the experimentally determined values of $\psi(x)$ by adjusting the only free parameter (the distance x) allows us to estimate the distances of the cis and trans entrances of the pore from the plane of the membrane, which are ≥ 5 nm and 0.5 nm, respectively, as reported in Table II.

We want to stress that these values are merely indicative because of the several assumptions we had to make in order to apply such general expressions as the GHK and GCS equations to a problem like a protein pore. Nevertheless we are confident that our main conclusion is correct: the two entrances of the pore are indeed located one near and one far from the plane of the membrane. This conclusion is corroborated by the digestion experiment shown in Fig. 6 and also by preliminary experiments with monoclonal antibodies which can modify the channel when added from the cis but not from the trans side (Ropele, M., unpublished result).

Acknowledgements

This work was financially supported by Italian CNR and MPI. We are indebted to S. Bhakdi for providing the hemolysin and the antibodies as well as for stimulating discussions. We also wish to thank F. Gambale for a critical reading of the manuscript.

References

1 Cavalieri, S.J., Bohach, G.A. and Snyder, I.S. (1984) Microbiol. Rev. 48, 326–343.
2 Welch, R.A., Dellinger, E.P., Minshew, B. and Falkow, S. (1981) Nature 294, 665–667.
3 Bhakdi, S., Mackman, N., Menestrina, G., Gray, L., Hugo, F., Seeger, W. and Holland, I.B. (1988) Eur. J. Epidemiol. 4, 135–143.
4 Mackman, N. and Holland, I.B. (1984) Mol. Gen. Genet. 199, 111–116.
5 Nicaud, J.-M., Mackman, N., Gray, L. and Holland, I.B. (1985) FEBS Lett. 187, 339–344.
6 Felmlee, T., Pellet, S. and Welch, R.A. (1985) J. Bacteriol. 163, 94–105.
7 Gonzalez-Carrero, M.I., Zabala, J.C., De la Cruz, F. and Oritz, J.M. (1985) Mol. Gen. Genet. 199, 106–110.
8 Bhakdi, S., Mackman, N., Nicaud, J.-M. and Holland, I.B. (1986) Infect. Immun. 52, 63–69.
9 Bhadki, S. and Tranum-Jensen, J. (1987) Rev. Physiol. Biochem. Pharmacol. 107, 147–223.
10 Menestrina, G., Mackman, N., Holland, I.B. and Bhakdi, S. (1987) Biochim. Biophys. Acta 905, 109–117.
11 Ludwig, A., Jarchau, T., Benz, R. and Goebel, W. (1988) Mol. Gen. Genet. 214, 553–561.
12 Menestrina, G. (1988) FEBS Lett. 232, 217–220.
13 Koronakis, V., Cross, M., Senior, B., Koronakis, E. and Hughes, C. (1987) J. Bacteriol. 169, 1509–1515.
14 Welch, R.A. (1987) Infect. Immun. 55, 2183–2190.
15 Glaser, P., Sakamoto, H., Bellalou, J., Ullmann, A. and Danchin, A. (1988) EMBO J. 7, 3997–4004.
16 Lo, R.Y.C., Strathdee, C.A. and Shewen, P.E. (1987) Infect. Immun. 55, 1987–1996.
17 Montal, M. and Mueller, P. (1972) Proc. Natl. Acad. Sci. USA 69, 3561–3566.
18 Menestrina, G. (1986) J. Membr. Biol. 90, 177–190.
19 Menestrina, G. and Ropele, M. (1989) Biosci. Rep., in press.
20 Apell, H.-J., Bamberg, E., Alpes, H. and Läuger, P. (1977) J. Membr. Biol. 31, 171–188.
21 Imoto, K., Busch, C., Sakmann, B., Mishina, M., Konno, T., Nakai, J., Bujo, H., Mori, Y., Fukuda, K. and Numa, S. (1988) Nature 335, 645–648.

22 Menestrina, G. and Porcelluzzi, C. (1986) Biochim. Biophys. Acta 856, 672–687.
23 Coronado, R., Rosenberg, R.L. and Miller, C. (1980) J. Gen. Physiol. 76, 425–446.
24 Schultz, S.G. (1980) Basic Principles of Membrane Transport, Cambridge University Press, New York, U.S.A.
25 Apell, H.-J., Bamberg, E. and Läuger, P. (1979) Biochim. Biophys. Acta 552, 369–378.
26 Bell, J.E. and Miller, C. (1984) Biophys. J. 45, 279–287.
27 Coronado, R. (1986) Annu. Rev. Biophys. Biophys. Chem. 15, 259–277.
28 Eisenmann, G. (1973) Membranes, Marcel Dekker, New York.
29 Lindemann, B. (1982) Biophys. J. 39, 15–22.
30 Nelson, A.P. and MacQuarrie (1975) J. Theor. Biol. 55, 13–27.
31 Bockris, J.O.M. and Reddy, A.K.N. (1970) Modern Electrochemistry, Vol. 1, Plenum Press, New York.
32 Richards, E.G. (1980) An introduction to physical properties of large molecules in solution, Cambridge University Press, New York.
33 Hille, B. (1984) Ionic channels of excitable membranes, Sinauer Associates Inc. Publishers, Sunderland, MA.
34 Delepierre, M., Dobson, C.M., Karplus, M., Poulsen, F.M., States, D.J. and Randall, E.W. (1987) J. Mol. Biol. 197, 111–130.
35 Sternberg, M.J.E., Hayes, F.R.F., Russell, A.J., Thomas, P.G. and Fersht, A.R. (1987) Nature 330, 86–88.
36 Eisenberg, M., Gresalfi, T., Riccio, T. and McLaughlin, S. (1979) Biochemistry 18, 5213–5223.
37 Tsui, F.C., Ojcius, D.M. and Hubbel, W.L. (1986) Biophys. J. 49, 459–468.